Electronic Supplementary Material (ESI) for Green Chemistry.

Ultrafast, Cost-Effective and Scaling-Up Recycling of Aramid Products into Aramid Nanofibers: Mechanism, Upcycling, Closed-Loop Recycling

Hui-Jun Chen, Qi-Yao Bai, Mei-Cheng Liu, Gang Wu* and Yu-Zhong Wang

Collaborative Innovation Center for Eco-Friendly and Fire-Safety Polymeric Materials (MoE), State Key Laboratory of Polymer Materials Engineering, National Engineering Laboratory of Eco-Friendly Polymeric Materials (Sichuan), College of Chemistry, Sichuan University, Chengdu 610064, China

E-mail: gangwu@scu.edu.cn

Table S1 The influence of different KOH form on preparation time

Solvent system	Volume of H_2O (mL)	Mass of KOH (g)	KOH form	Volume of DMSO (mL)	Concentration of ANFs (wt%)	Preparation time
KOH/ DMSO	0	0.15	Untreated flake	50	0.2	6 days
	0	0.15	Ground powder	50	0.2	16 h
KOH/ H_2O/ DMSO	2	0.15	Untreated flake	50	0.2	4 h
	2	0.15	Ground powder	50	0.2	1 h

Reaction conditions: KOH was ground then passed through a sieve with 50 mesh. KOH was fully dried at 100 °C before used. DMSO was used as received. The order of adding KOH, H_2O, aramid fibers into DMSO has no significant effect on the preparation time in KOH/H_2O/DMSO.

Table S2 Different volume ratios of H_2O to DMSO

Volume of H_2O (mL)	H_2O:DMSO (mL:mL)	Mass of KOH (g)	Concentration of KOH in H_2O (g mL^{-1})	Volume of DMSO (mL)	Concentration of ANFs (wt%)
0.25	1:200	0.15	0.6	50	0.2
0.5	1:100	0.15	0.3	50	0.2
1	1:50	0.15	0.15	50	0.2
1.5	3:100	0.15	0.1	50	0.2
2	1:25	0.15	0.075	50	0.2
2.5	1:20	0.15	0.06	50	0.2
3	3:50	0.15	0.05	50	0.2
4	2:25	0.15	0.0375	50	0.2
5	1:10	0.15	0.03	50	0.2

The amount of KOH remains constant throughout the system. All reactions are carried out in a 100 mL flask at room temperature.

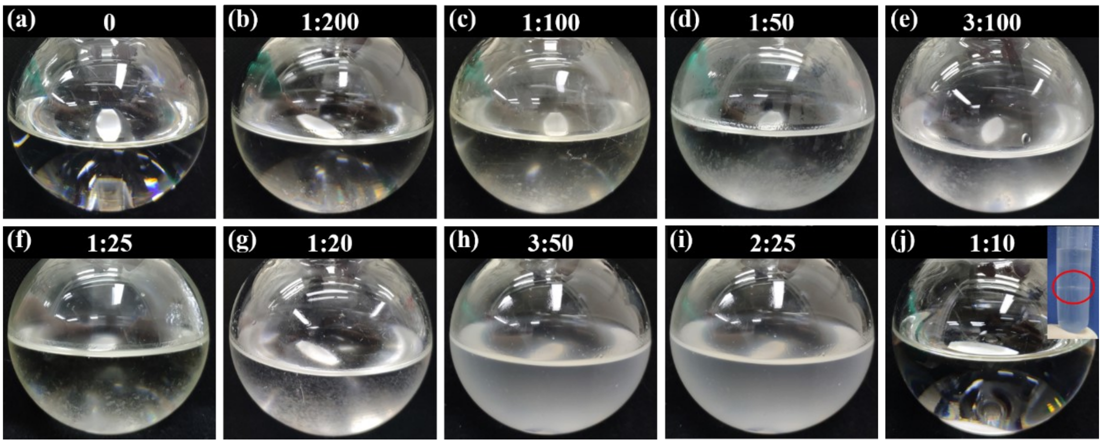

Fig. S1 Digital photo of KOH(aq)/DMSO system with different volume ratios of H_2O to DMSO. The KOH solution and DMSO formed an emulsion when the ratio was further increased to 3:50 and 2:25. The KOH solution and DMSO stratified when the ratio was further increased to 1:10. The illustration in (j) is a digital photo of the zoom-in experiment at this scale.

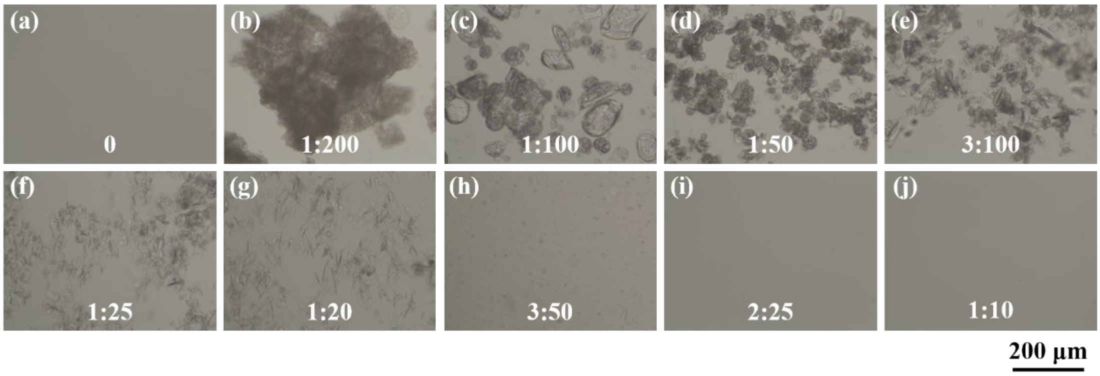

Fig. S2 Photos of KOH precipitate with different volume ratios of H_2O to DMSO, which observed under optical microscope.

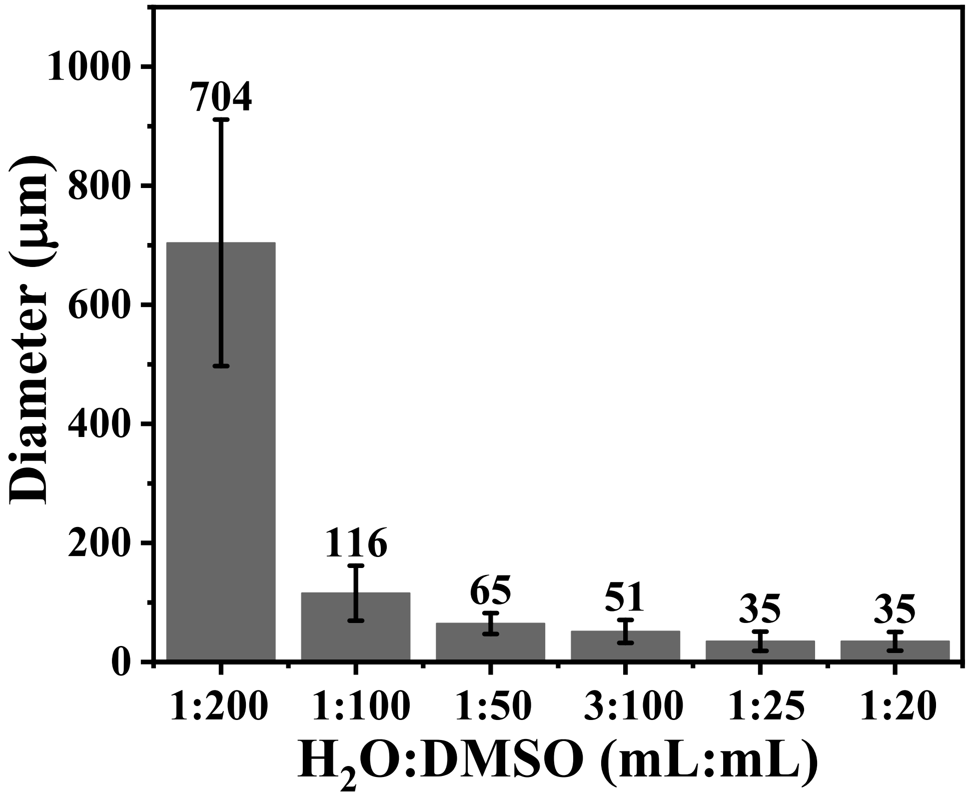

Fig. S3 The diameter statistics of KOH precipitate with different volume ratios of H_2O to DMSO.

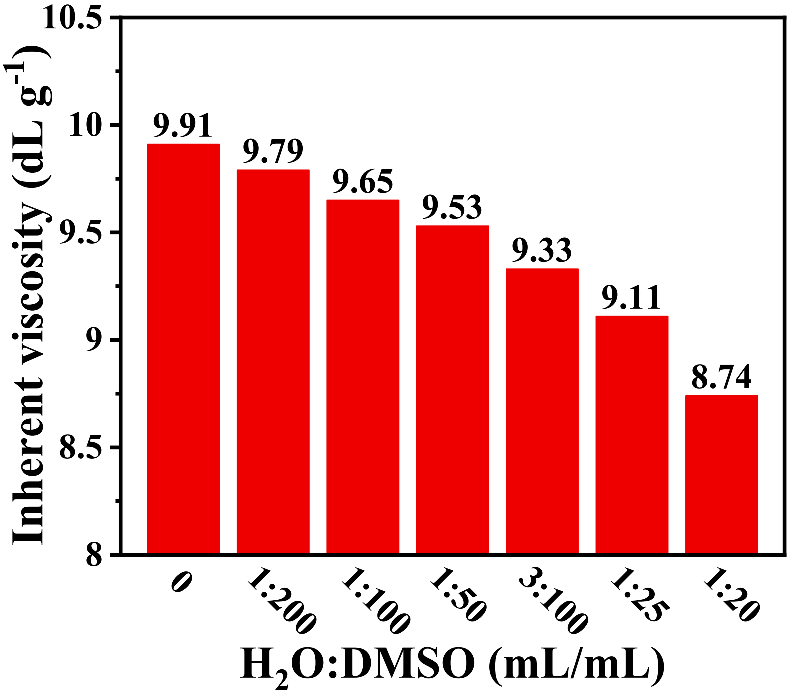

Fig. S4 Inherent viscosity of ANFs with different volume ratios of H_2O to DMSO.

The inherent viscosity of ANFs/DMSO solution was determined by a Ubbelohde viscometer. The capillary tube diameter was 0.6-0.7 mm, and the temperature of the water bath was 30 ± 0.1 °C

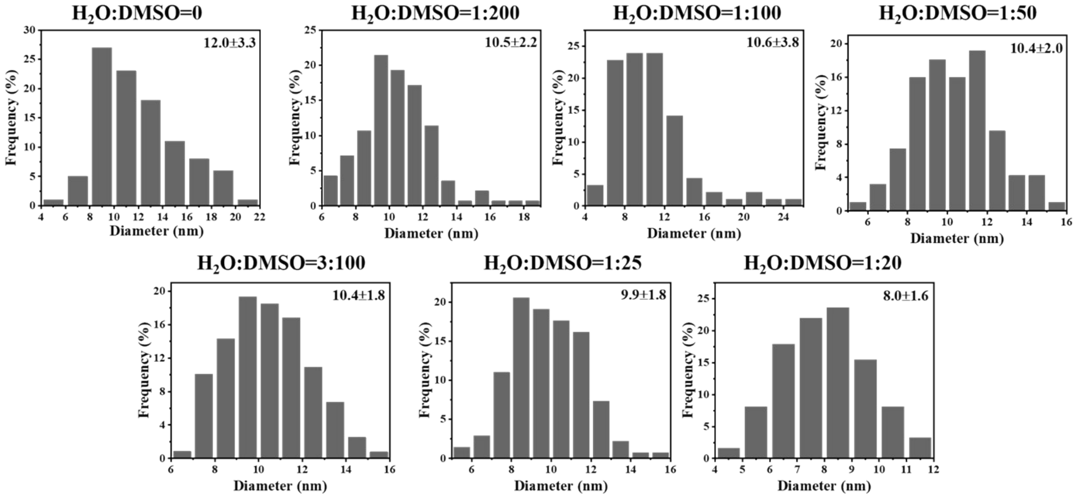

Fig. S5 The diameter distribution for ANFs dispersions with different volume ratios of H_2O to DMSO

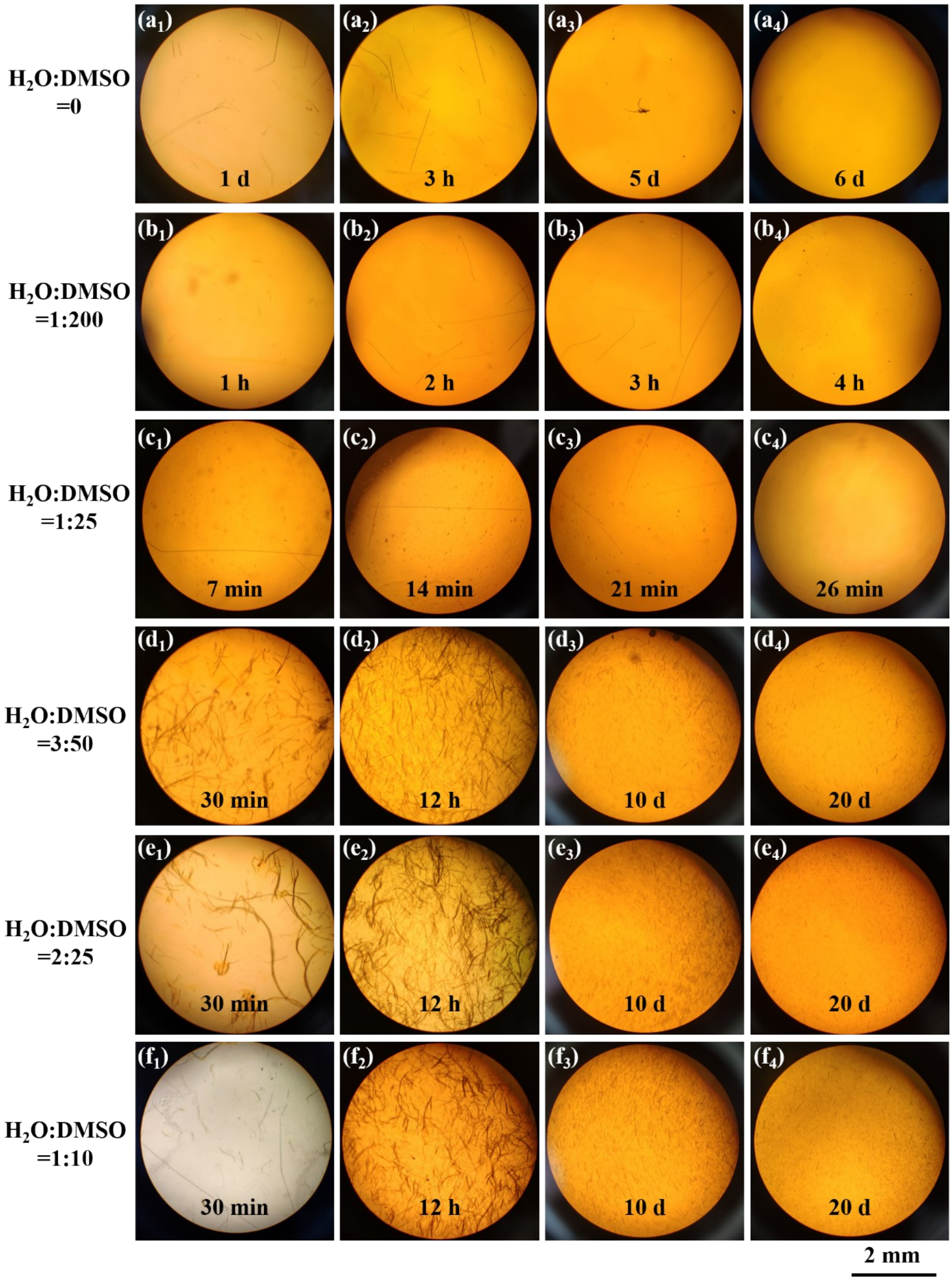

Fig. S6 Digital photos during ANFs formation which observed under optical microscope. When the volume ratio of H_2O to DMSO was 3:50, 2:25 and 1:10, macroscopic aramid fibers can still visible in the system even after 20 days

Table S3. Different mass ratios of KOH to aramid fibers

Volume of H_2O (mL)	Mass of KOH (g)	KOH:Aramid fibers (g:g)	Concentration of KOH in H_2O (g mL^{-1})	Volume of DMSO (mL)	Concentration of ANFs (wt %)
2	0.06	3:5	0.03	50	0.2
2	0.075	3:4	0.0375	50	0.2
2	0.1	1:1	0.05	50	0.2
2	0.15	3:2	0.075	50	0.2
2	0.3	3:1	0.15	50	0.2
2	0.6	6:1	0.3	50	0.2
2	0.8	8:1	0.4	50	0.2
2	1	10:1	0.5	50	0.2
2	1.2	12:1	0.6	50	0.2

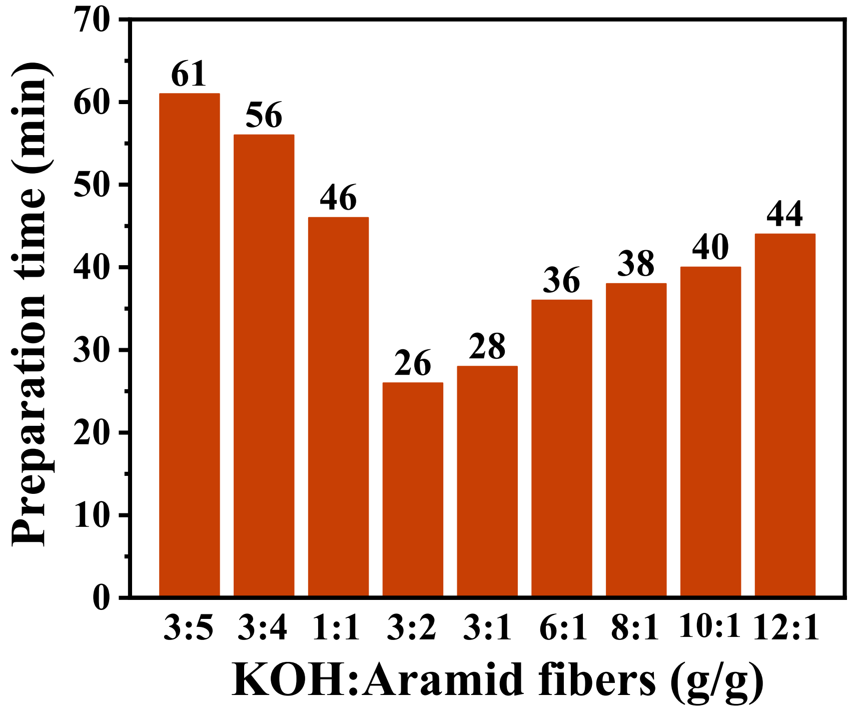

Fig. S7 Preparation times of ANFs with different mass ratios of KOH to aramid fibers

Table S4 Summary of ANFs preparation methods

<table>
<tr><td colspan="2">Preparation Method</td><td>Product Forms</td><td>Diameter of ANFs</td><td>Energy Consumption</td><td>Operability</td><td>Preparation time (Concentration)</td><td>Ref.</td></tr>
<tr><td>Bottom-up strategy</td><td>Polymerization induced self-assembly</td><td>ANFs/H_2O dispersions</td><td>~20-50 nm</td><td>Low</td><td>Low</td><td>n.a. (3 wt%)</td><td>1</td></tr>
<tr><td rowspan="11">Top-down strategy</td><td>Electrospinning</td><td>Fibers</td><td>275 nm-15 μm</td><td>High</td><td>Low</td><td>~4 h (n.a.)</td><td>2</td></tr>
<tr><td>Immersion rotary jet-spinning</td><td>Fibers</td><td>500-1000 nm</td><td>Medium</td><td>Low</td><td>n.a.</td><td>3</td></tr>
<tr><td>Alkaline hydrolysis pretreatment mechanical disintegration</td><td>Precipitate</td><td>10-200 nm</td><td>High</td><td>Low</td><td>n.a. (1 wt%)</td><td>4</td></tr>
<tr><td>KOH/DMSO (Deprotonation)</td><td>ANFs/DMSO dispersions</td><td>3-30 nm</td><td>Low</td><td>High</td><td>7 days (0.2 wt%)</td><td>5</td></tr>
<tr><td>EtOK/DMSO (Deprotonation)</td><td>ANFs/DMSO dispersions</td><td>2-9 nm</td><td>Low</td><td>High</td><td>7 days (1 wt%)</td><td>6</td></tr>
<tr><td>t-BuOK/DMSO (Deprotonation)</td><td>ANFs/DMSO dispersions</td><td>~9-18 nm</td><td>Low</td><td>High</td><td>7 days (0.5 wt%)</td><td>7</td></tr>
<tr><td>t-BuOK/MeOH/DMSO (Proton donor-assisted deprotonation)</td><td>ANFs/DMSO dispersions</td><td>~3-14 nm</td><td>Low</td><td>Medium</td><td>n.a. (10 wt%)</td><td>8</td></tr>
<tr><td>Fibrillation pretreatments deprotonation</td><td>ANFs/DMSO dispersions</td><td>12-17 nm</td><td>High</td><td>Low</td><td>3 days (0.2 wt%)</td><td rowspan="3">9</td></tr>
<tr><td>Ultrasonication pretreatments deprotonation</td><td>ANFs/DMSO dispersions</td><td>10-14 nm</td><td>Medium</td><td>Medium</td><td>24 h (0.2 wt%)</td></tr>
<tr><td>KOH/H_2O/DMSO (Proton donor-assisted deprotonation)</td><td>ANFs/DMSO dispersions</td><td>10-12 nm</td><td>Low</td><td>High</td><td>4 h (0.2 wt%)
12 h (4 wt%)</td></tr>
<tr><td>**KOH(aq)/DMSO**</td><td>**ANFs/DMSO dispersions**</td><td>**8-12 nm**</td><td>**Low**</td><td>**High**</td><td>**26 min (0.2 wt%)**
10 h (4 wt%)</td><td>**This work**</td></tr>
</table>

Table S5 Wavenumbers and vibration types of aramid fibers and ANFs in Raman scattering.

Aramid fibers ν, (cm^{-1})	Assignment	ANFs ν (cm^{-1})
627	Ring vibrations	disappear
729	Ring vibrations	disappear
785	Ring vibrations	disappear
843	C-H out-of-plane bending	839
1099	C-H in plane bending	1093
1180	C-C ring stretching	1155
1277	C-C ring stretching	1261
1327	C-C ring stretching	1352
1516	C-C ring stretching	1529
1568	Amide II (60% N– H bending, 40% C-N stretching)	1574
1608	C–C ring stretching	1597
1647	Amide I (80% C=O stretching, 10% N-H bending, 10% C-N stretching)	disappear

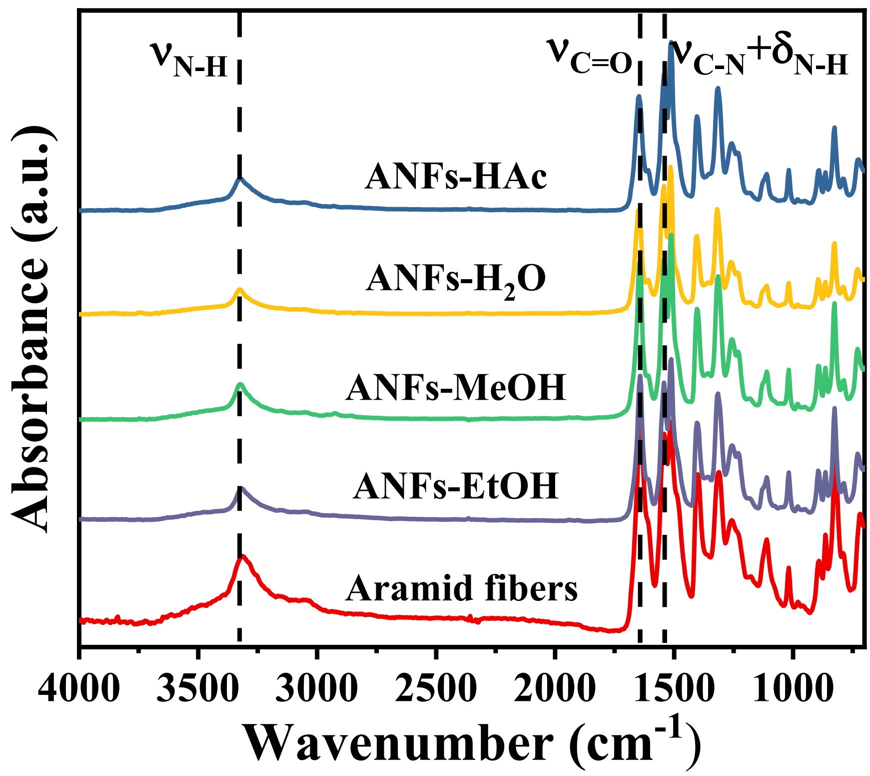

Fig. S8 FT-IR spectra of ANFs-HAc, ANFs-H_2O, ANFs-MeOH, ANFs-EtOH aerogel and aramid fibers

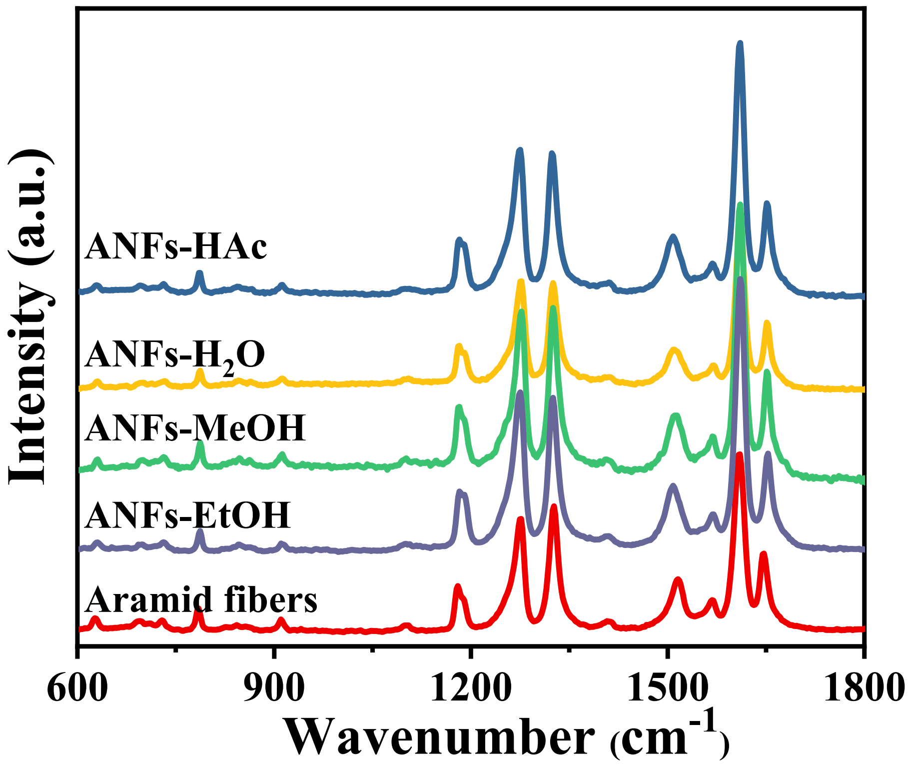

Fig. S9 Raman scattering of ANFs-HAc, ANFs-H_2O, ANFs-MeOH, ANFs-EtOH aerogel and aramid fibers

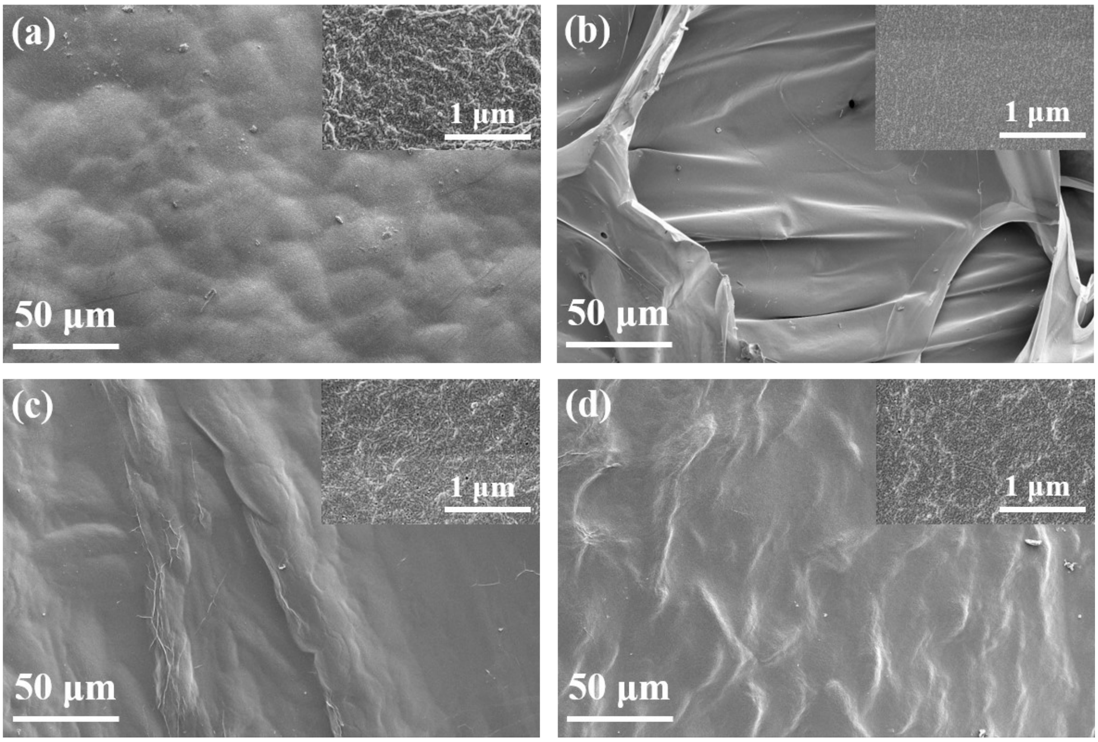

Fig. S10 SEM images of the upper surface of (a) ANFs-HAc, (b) ANFs-H_2O, (c) ANFs-MeOH and (d) ANFs-EtOH aerogel

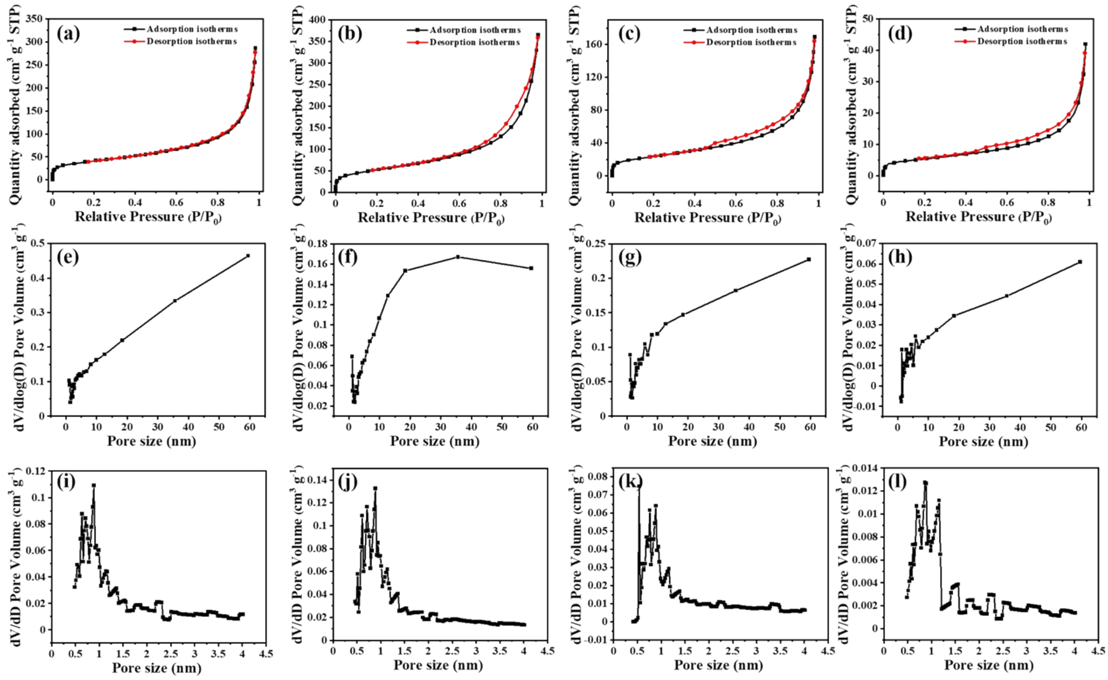

Fig. S11 (a-d) Nitrogen adsorption-desorption isotherms of ANFs-HAc, ANFs-H_2O, ANFs-MeOH and ANFs-EtOH aerogel, respectively. (e-h) Pore size distribution of mesopores of ANFs-HAc, ANFs-H_2O, ANFs-MeOH and ANFs-EtOH aerogel (BJH method), respectively. (i-l) Pore size distribution of micropores of ANFs-HAc, ANFs-H_2O, ANFs-MeOH and ANFs-EtOH aerogel (SF method), respectively.

Table S6 Surface area, pore volume and pore size data of ANF aerogels

Sample	S_{BET} (m^2/g)	BJH pore volume (cm^3/g)	SF pore volume (cm^3/g)	Pore size (nm)
ANFs-HAc	144.9	0.44	0.083	6.84
ANFs-H_2O	184.8	0.56	0.107	7.53
ANFs-MeOH	85.0	0.26	0.049	7.13
ANFs-EtOH	18.8	0.06	0.011	11.50

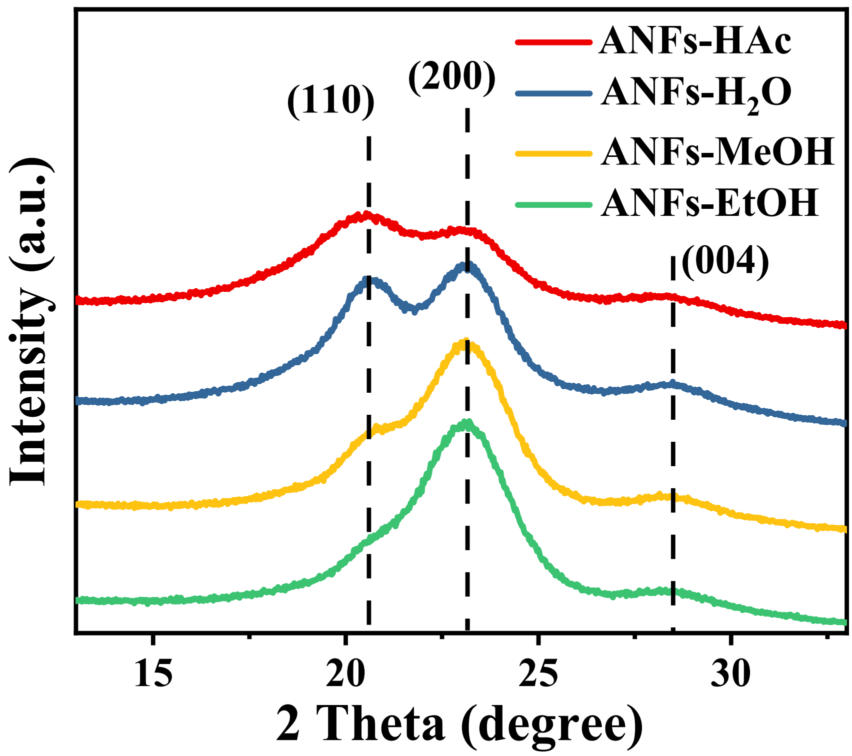

Fig. S12 XRD pattern of ANFs aerogels

Table S7 TGA-DTG data of aramid fibers and ANFs aerogels

Sample	Temperature of 10% weight loss, T_d (°C)	Peak decomposition temperature, T_{max} (°C)	Residual weight at 700 °C (%)
Aramid fibers	571.8	590.1	49.2
ANFs-HAc	542.5	573.1	47.5
ANFs-H_2O	538.9	575.1	48.8
ANFs-MeOH	534.0	572.5	46.7
ANFs-EtOH	535.1	574.5	48.2

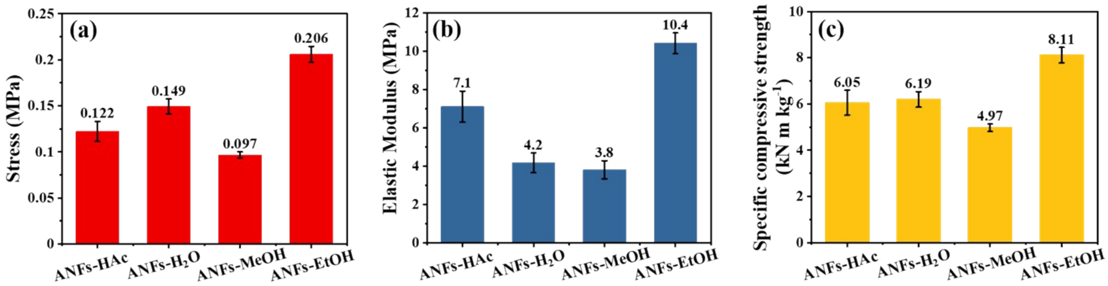

Fig. S13 (a) Compressive stress (ε = 70%) comparison of ANFs aerogels. (b) Elastic modulus comparison of ANFs aerogels. (c) Specific compressive strength of ANFs aerogels.

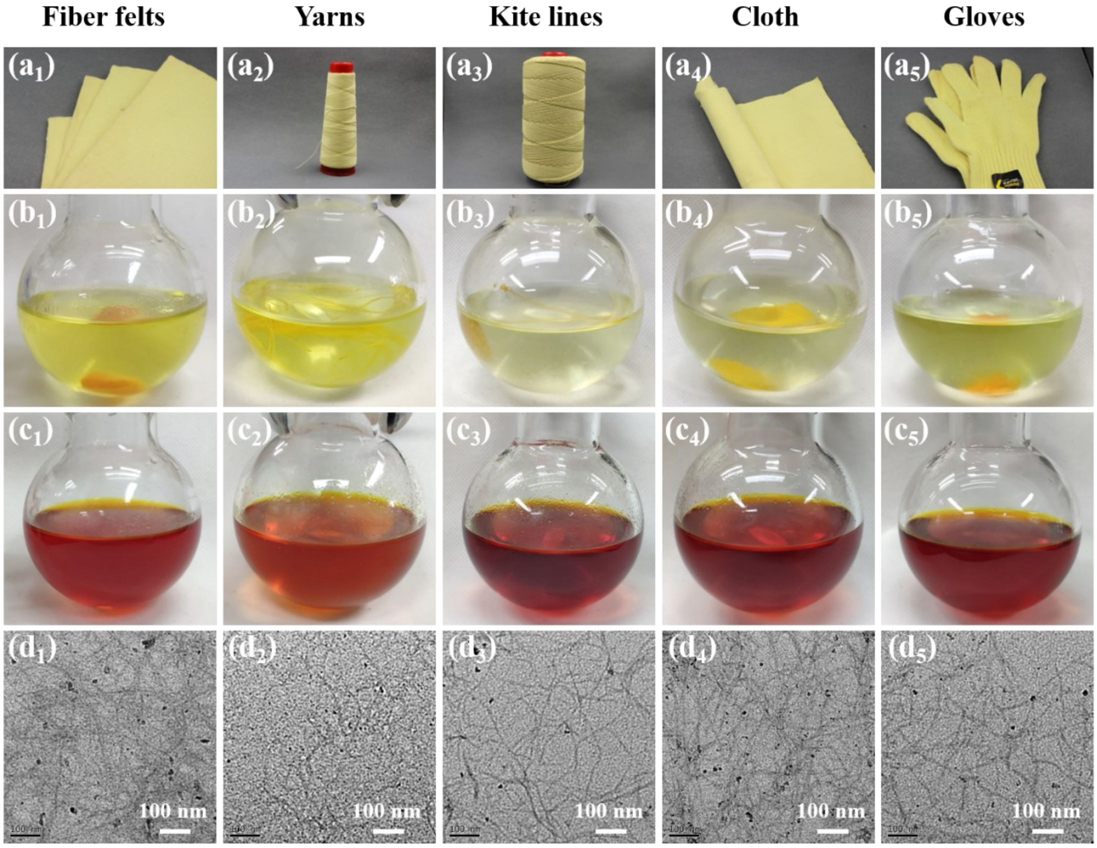

Fig. S14 (a_1-a_5) Digital photos of Kevlar products. (b_1-c_5) Digital photos of the deprotonation process in KOH(aq)/DMSO system to obtain 0.2 wt% ANFs dispersions. (d_1-d_5) TEM images of ANFs prepared from different aramid products.

REFERENCES

1. H. Yan, J. Li, W. Tian, L. He, X. Tuo and T. Qiu, *RSC advances*, 2016, **6**, 26599-26605.
2. J. Yao, J. Jin, E. Lepore, N. M. Pugno, C. W. Bastiaansen and T. Peijs, *Macromolecular Materials and Engineering*, 2015, **300**, 1238-1245.
3. G. M. Gonzalez, L. A. MacQueen, J. U. Lind, S. A. Fitzgibbons, C. O. Chantre, I. Huggler, H. M. Golecki, J. A. Goss and K. K. Parker, *Macromolecular Materials and Engineering*, 2017, **302**, 1600365.
4. S. Ifuku, H. Maeta, H. Izawa, M. Morimoto and H. Saimoto, *RSC Advances*, 2014, **4**, 40377-40380.
5. M. Yang, K. Cao, L. Sui, Y. Qi, J. Zhu, A. Waas, E. M. Arruda, J. Kieffer, M. Thouless and N. A. Kotov, *Acs Nano*, 2011, **5**, 6945-6954.
6. J. Zhu, M. Yang, A. Emre, J. H. Bahng, L. Xu, J. Yeom, B. Yeom, Y. Kim, K. Johnson and P. Green, *Angewandte Chemie International Edition*, 2017, **56**, 11744-11748.
7. S. Hu, S. Lin, Y. Tu, J. Hu, Y. Wu, G. Liu, F. Li, F. Yu and T. Jiang, *Journal of Materials Chemistry A*, 2016, **4**, 3513-3526.
8. W. Cao, L. Yang, X. Qi, Y. Hou, J. Zhu and M. Yang, *Advanced Functional Materials*, 2017, **27**, 1701061.
9. B. Yang, L. Wang, M. Zhang, J. Luo and X. Ding, *ACS nano*, 2019, **13**, 7886-7897.